SOLIDIFICATION MODELING IN COPPER CONTINUOUSLY CAST IN GRAPHITE MOULDS

R. Ghasemzadeh And S. H. Algie***

* Metallurgy Dept., Iran University of Science and Technology Narmak, Tehran, Iran.
** Department ot Mining and Metallurgical Engineering University of Queensland. Brisbane. Australia.

Received November 1988

Abstract A mathematical model of heat transfer in continuous casting copper slabs capable of producing experimental data has been constructed and validated against experimental data provided by the management of Copper Refineries Ltd., Townsville plant in Australia. It has been used to predict the effects of major casting variables; metal temperature, casting speed and metal conductivity. The results can be expressed most conveniently through their effects on predicted depth of liquid pool.

چکیده الگوی ریاضی بر مبنای حرارت منتقل شده از شمشالهای مس در حین ریختن مداوم آن به گونه‌ای در این مقاله تدوین شده که قادر به ارائه نتایج عملی میباشد. پس از تدوین الگو آنرا با داده‌های تجربی حاصل از خط تولید مس کارخانه تانزویل استرالیا تطبیق داده تا نتایج حاصل از آن معتبر گردد. آنگاه اثرات متغیرهای اصلی منجمله دمای فلز، سرعت ریختن و هدایت حرارت فلز روی عمق مخروط قالب بررسی شده‌است، نتایج حاصل‌را میتوان با اعتماد بکار برد. تجربیات اضافی وگسترش هر چه بیشتر این الگو راه را برای طراحی مناسب سیستم فراهم میکند.

INTRODUCTION

Solidification can be modelled mathematically through the establishment of a heat balance about the solid/liquid interface. In the solidification process there is a continuous change in position of the solid/liquid interface so that the mathematical calculation of solidification is a moving boundary problem and potentially complex. The effect of forced and natural convective heat transfer within the liquid pool on the solid-liquid interface for pure metals has, however, been shown to be very small[1]. Therefore, relative motion between the liquid and solid phases may be neglected. This simplifying assumption allows a single energy equation to be applied simultaneously over both the liquid and solid regions of the ingot.

Mathematical model

In the continuous casting process used at Copper Refineries Ltd., the slab passes through three distinct zones of cooling as follows:

a) cooling by heat transfer to the mould wall.

b) forced convection cooling by water sprays.

c) cooling by heat transfer to the environment by convection or radiation.

The region of heat transfer to the mould wall is further divided into two zones.

a) From top surface to the point where the solid shell contracts away from the wall. In this region the heat transfer co-efficient is high.

b) The region over which the solid shell pulls away, to form a gap between the

casting and the mould. In this region the heat transfer coefficient is low.

THEORY

Many theoretical and experimental investigations have been directed towards a more profound understanding of the continuous casting process. Starting with the studies of Mizikar[2],the majority of work has been done on steel in search of a mathematical model describing the temperature profile over the ingot during solidification and the approach used here is based on these studies.

The conduction of heat in a medium moving at velocity v in direction z with the realistic assumption that the longitudinal thermal flow is negligible[3], reduces the heat transfer problem to a two dimensional one with transfer in the x and y directions only, so that a planar cross section (or nodal slice) can be considered during its translation through the mould. This is represented by the following equation.

$$\nabla^2 (KT) = \rho C_p \frac{\partial T}{\partial t} \qquad (1)$$

where

∇ = gradient operator
K = K(T) isotropic conductivity coefficient
T = T(x, y, t) = unknown temperature field
$\rho = \rho$ (T) = mass density
$C_p = C_p(T)$ = specific heat capacity
t = time

From this equation the temperature distribution in the solid metal can be obtained subject to the initial temperature distribution and the boundary condition at the periphery of the slice where heat (enthalpy) is transferred to the surroundings.

$$\frac{dH}{A\,dt} = h(T_s - T_{env} \qquad (2)$$

where

H = enthalpy
h = heat transfer coefficient
A = area for heat transfer
T_s = surface temperature of metal
T_{env} = Temperature of surroundings

The additional problem introduced by the change of phase is the latent heat (enthalpy of fusion) which is evolved at the solid/liquid interface. There are various ways of incorporating this into the solution. One way is to express a pseudo specific heat as a function of temperature around the melting point such that its integration over this limited temperature range is equal to the latent heat. The simpler alternative, adopted here, is to express equation 1 in terms of enthalpy

$$\nabla^2 (KT) = \frac{\partial H}{\partial t} \qquad (3)$$

From a known metal temperature distribution at time t, the enthalpy H_t is calculated from a knowledge of enthalpy temperature relationship. Using it as an initial value at time t, the temperature and enthalpy distribution and at time $t+\Delta t$ can be calculated using equations 1 and 3 using a finite difference technique. For both liquid and solid regions the enthalpy $H_{t+\Delta t}$ distribution at each time increment and the temperatures $T_{t+\Delta t}$ at time $t+\Delta t$ can be calculated and the calculated cycle repeated[4,5].

The slab geometry casting speed together with the incoming copper temperature are used to set up the initial values in the nodal slice at zero time.

PROCEDURE

The representative nodal slice of metal is divided into a number of smaller elements. Each element is represented by a node which is located at the centre of the element. The finite difference method is applied to calculate the enthalpies at all nodal points other than line and corner boundaries, using appropriate

heat flux equations. Here the problem is made equivalent to one of the non-linear heat conduction without change of phase. Temperatures at surface nodes are set by the external heat transfer coefficients. This process is then repeated for successive nodal slices until the chosen temperature or time is reached. Equations for all nodes are given in the appendix.

In the present work Δx is chosen to be equal to Δy. As the increments of Δt and Δx are made smaller the solution becomes more accurate but the time increments must be chosen depending on the value of the thermal diffusivity, α, otherwise the solution becomes unstable. The criterion of stability is to make the value $(\Delta x)^2/\alpha . \Delta t \geq 4$.

The major difficulty in the numerical analysis of the continuous casting process is the accuracy of boundary conditions. Here the conduction of heat through the mould region is calculated using experimental heat transfer coefficients derived from full scale casting. The characteristics of the heat transfer in the spray region area are very complex, since it is influenced by parameters such as spray intensity, nozzle type, spray angle and nozzle postion. Heat transfer coefficients for cooling with nozzles with different opening diameters and various water pressures have been correlated by Bamberger and Prinz[6]. These are a function of water spray intensity and cooling water temperature [7,8]. The influence of impact velocity was found to be minor[9] for stable film boiling condition at smooth surfaces.

Although there are several empirical factors to be considered in calculating heat transfer coefficients, the overall validity of the model may be assessed by comparison in the experiment. If the model fits, then its predictions should be reasonable provided the conditions are not extrapolated too far from those for which it has been tested.

Thermophysical data

The specifications for casting are as follows[10].

1. Oxygen content of copper analysis was between 0.020 to 0.40%. Its purity was approximately 99.97%. Therefore the metal can be assumed to be pure.
2. Copper temperature was controlled in the induction furnace in the range of 1140 - 1190°C. A temperature of 1170°C is common. Initially metal is delivered to the mould 20-30°C lower, but was measured to be 1088°C in the mould once casting had settled down.
3. Ambient temperature was between 28 - 40°C depending on prevailing weather conditions, an average value was 34°C.
4. Casting rates were variable, but a withdrawal speed of 0.0044 m sec^{-1}(10.5 inch/min) was chosen for evaluation of data.
5. The product size and mould shape used in model evaluation was 0.15 ×0.65 m.

The enthalpy, thermal conductivity, specific heat and the density of copper as a function of temperature for two different zones were taken as follows[11,12].

(1) Solid (298 - 1357)K

$$H = H_T - H_{298} = -1680 + 5.41T + 0.75 \times 10^3 T^2 \text{cal.mole}^{-1}$$

$$K = 1.01 - 0.00016T \text{ cal.cm}^{-1} \text{s}^{-1} \text{K}^{-1}$$

$$C_p = 5.41 + 1.5 \times 10^3 T \text{ cal.K}^{-1} \text{mole}^{-1}$$

$$\rho = 8890 - 570 . (T - 293)/1063 = -9047 - 0.54 T \text{kg.m}^{-3}$$

(2) Melt (1357 - 1600) K

$$H = H_T - H_{298} = 20 + 7.5T \text{ cal.mole}$$

$$K = 0.04 \text{kcalm}^{-1} \text{s}^{-1} \text{K}^{-1}$$

$$C_p = 7.5 \text{cal.K}^{-1} \text{mole}^{-1}$$

$$\rho = 7930 \text{kg.m}^{-3}$$

The heat transfer coefficients in the mould-shell interface in the three zones were considered to be 0.5, 0.2 and 0.3 kcal.$m^{-2}.s^{-1}.K^{-1}$ respectively.

The heat transfer coefficient represented by the water spray cooling was extracted from data given by Bamberger and Prinz [6] and

depends only on surface temperature. The heat transfer coefficient was fitted to a curve of the form:

$$h = a_0 + a_1 T_c \quad a^2 + \quad + a_3 T_c^3 \, a_4 T_c^4$$

Experimental Determination of Heat Transfer Coefficient

Heat transfer coefficients were estimated from measurements on the liquid metal pool geometry with supplementary confirmation from temperature measurements within the graphite mould.

The liquid pools in 0.65 x 0.15 m slabs were measured by adding about 150 g of solid tin to the liquid just before the end of the cast. The liquid froze very rapidly after the tin addition, since the slabs are cast with very low superheat. The measured liquid pool temperature of 1088°C is only 4°C above the freezing point of copper and the difficulty in obtaining a measurement confirmed the smallness of this margin. The end of the slab was sectioned through the centre longitudinally and transversally, etched and examined macroscopically.

The liquid pool profile was indicated by a change in colour and, in some cases by a change from columnar to small equiaxed grains. For the most part the interface could be located objectively, but in some regions, especially near the top, it was less distinct. There is some uncertainty in fixing distances below the liquid surface at the time of the tin addition since the top of the slab showed the usual slightly domed pattern. The growth direction of the columnar grains was at all stages perpendicular to the indicated solid/liquid interface.

The end wall of the mould was fitted with thermocouples in holes drilled parallel to and 6 mm in from the hot face and at right angles to the axis of the mould. The first was 0.5 inch (12.7 mm) from the top of the mould and ten others were fitted at 1.25 inch (30 mm) intervals below the first. The thermocouples were directly in line with, and 17 mm from, the nearest front on the vertical water cooling tubes. The cooling water exit temperature was also measured.

The solid-liquid interface parallel to the long side of the slab (Figure 1) shows three distinct regions characterised by differing values

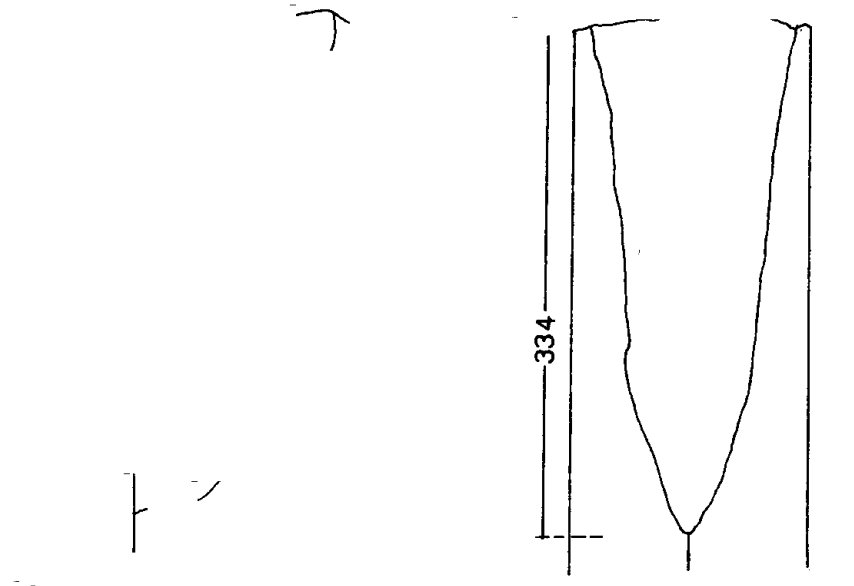

Figure 1: Cross sections through 650 × 150 mm slab cast at 10% inch min1

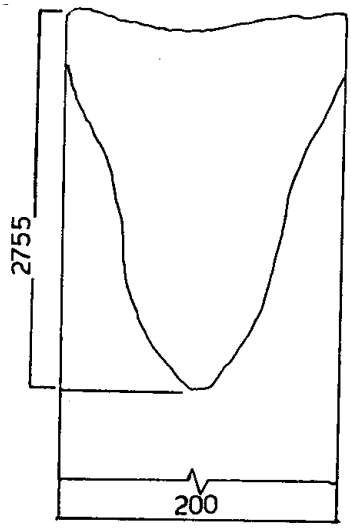

CROSS SECTION THROUGH 200 mm DIA BILLET CAST AT 10 INCH MIN^{-1}

Figure 2: Cross section through 200 mm dia billet cast at 10 inch min^{-1}

of the rate of change dx/dz of solid thickness, x, with distance below the top of the liquid pool, z; within each region the rate of change was approximately constant. The pattern was quite general and was also seen in profiles obtained perpendicular to the long side and with round billets (see Figure 2). Since the superheat is very small and the rate of growth of the solid wall is proportional to the rate of heat removal, the assumption that the only significant direction of heat flow is perpendicular to the mould wall allows the calculation of heat flux from the liquid/solid profile.

The heat removal from the melt can be calculated using a heat balance in the solid/liquid interface. The volume frozen over a thickness l, per unit width, when the solid/liquid interface advances $\triangle x$ is

$$\triangle V = x.\triangle l = \frac{dx}{dz} \triangle \quad \triangle$$

The time to freeze is:

$$\triangle t = \frac{\triangle l}{v}$$

where v is the casting speed and therefore $\triangle l = v.\triangle t$. The mass frozen is

$$\triangle m = \rho \triangle V$$

Where ρ is the density of the metal and hence the heat removed is

$$\triangle H = L \triangle m$$

where L is the latent heat of freezing per unit mass.

From this the heat flux in the slice is

$$\frac{dH}{\quad} = \frac{\triangle H}{\quad}$$

or

$$\frac{dH}{A.dt} = L.\rho \frac{dx}{dz}.v$$

where dx/dz represents the gradient of the liquid pool with increasing distance from the top of the mould.

Using this equation the heat flux values were estimated for a casting speed of 0.0044 m.s^{-1} (10.5 inch per min) from the profiles shown in Figure 1. The value of latent heat used was 228 kj kg^{-1} and density was taken to be 8900 kg m^{-3}.

These flux values allowed the estimation of the overall heat transfer coefficient (h) between the surface of the solid slab and the cooling water.

$$\frac{dH}{A.dt} = \frac{T_L - T_w}{\frac{x}{K} + \frac{1}{h}} \qquad 5$$

The temperature at the solid/liquid interface T_L is the freezing temperature of copper, taken to be 1084°C. The temperature of the exit cooling water, T_w, was measured in the range 39 to 40°C; the inlet water was at 37°C. The representative value was taken as 40°C. The thermal conductivity of copper used was 380 W.m^{-1}.K^{-1}, and x represents the thickness of solid copper. The values obtained are shown in the Table 1.

In these calculations the transition from one region to another has been treated as a discontinuous change. This is clearly an approximation.

Table 1.

Region	Distance from top (m)	x (m)	dx/dy	q MW. m^{-2}	h MW. $m^{-2}K^{-1}$
1	from 0	0	0.21	1.88	1.80
	to 0.1	0.025	0.21	1.88	2.04
2	from 0.1	0.025	0.09	0.80	0.81
	to 0.25	0.04	0.09	0.80	0.84
3	from 0.25	0.04	0.38	3.39	4.94
	to 0.35	0.075	0.38	3.39	9.06

The temperature measurements in the graphite mould were of limited use in determining heat transfer coefficients. At each point of measurement the temperature fluctuated as the level of the liquid in mould varied around the nominal value of about 40 mm from the top. Any fluctuations in temperature were observed to pass down the series of the thermocouple at the casting speed. The only temperature measurement which was of direct use in the estimation of heat transfer was the highest value observed at each point during a cast. The values were logged at various set intervals during the test but a maximum value of at least about 370°C is considered representative and such values were observed with thermocouples located at 43, 74 and 104 mm from the top of the mould. These must have occurred at times when the mould at that distance from the top must have been adjacent to a very thin shell of metal.

The heat flux in the mould wall may be estimated as follows:

$$\frac{dH}{A.dt} = K_g \frac{T_M - T_W}{x} \qquad 6$$

where T_M is the measured temperature, K_g is the conductivity of graphite and x is the distance between the thermocouple and the cooling tube (17 mm). Substituting appropriate values, using $K_g = 112\ W.m^{-1}\ K^{-1}$

$$\frac{dH}{A.dt} = 2.17\ MW.m^{-2}$$

This is in good agreement with the flux of 1.88 $MW.m^{-2}$ in the first region calculated from the liquid/solid profile and so supports the estimate of heat transfer coefficient made there.

Since the calculated heat transfer coeffi-

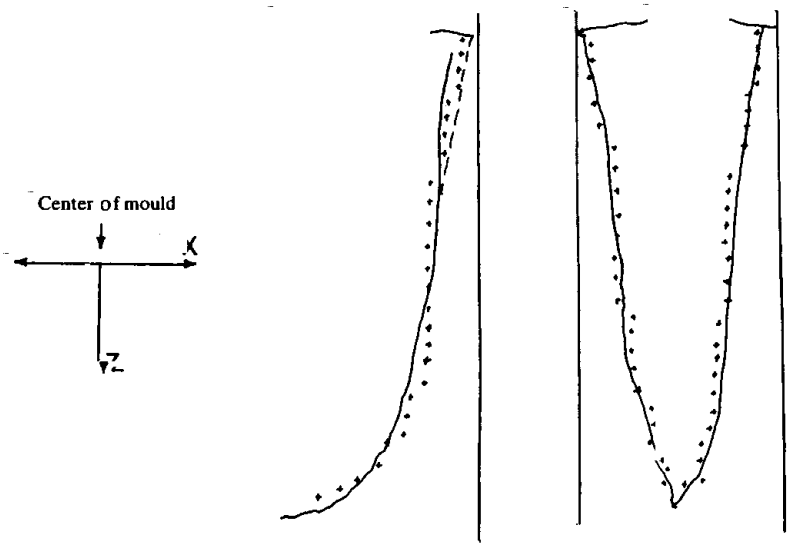

Figure 3: Messured(–)and calculated(+)liquid pool profiles (1 cm computational grid)

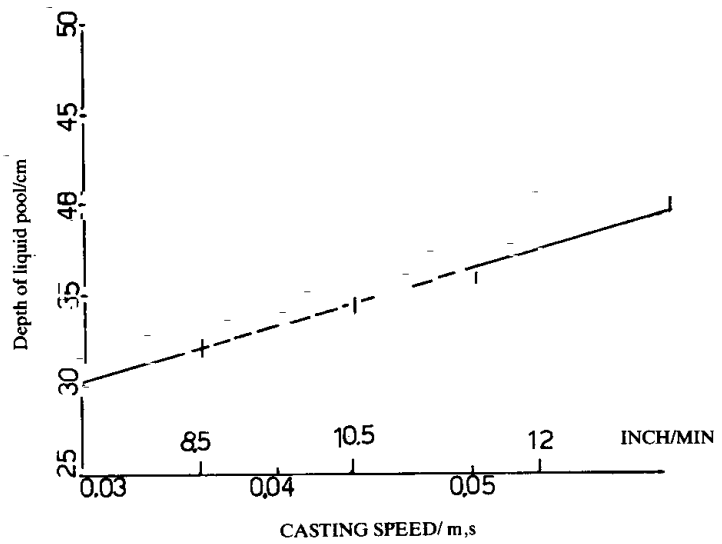

Figure 4: Effect of casting speed on liquld pool depth 650×150 mm slab. 1088 deg.C

cients do not show a great variation within each region a single value was accepted for each region in the calculations. Using the experimental coefficients as a starting point, values were fitted by trial and error until the calculated and experimental liquid pool profiles were in close agreement as shown in Figure 3. The marked points represent the location of the last liquid cell centre in the computational grid.

THE SURFACE HEAT TRANSFER COEFFICIENT

Although it is not required in the calculation, the heat transfer coefficient, h_g, between the metal surface and the mould surface may also be estimated from the overall heat transfer coefficients by making allowance for the thermal resistance of the mould wall in the 23 mm thickness between the surface and the cooling passages. The results are shown in Table 2.

Table 2.

Region	x (m)	h_g(kW.m^{-2}K^{-1})
1	0	2.86
	0.025	3.52
2	0.025	0.97
	0.04	1.01

The first region is taken to be characteristic of good contact between the solidifying metal and the mould. The second is interpreted as representing transfer across a gap which is opened by shrinkage of the solidifying metal. In both regions the heat transfer coefficient is at least an order of magnitude greater than that for heat transfer purely by radiation between the two surfaces.

At the end of casting a zone of discoloration of the graphite mould is evident some 200 to 250 mm from the top of the mould. This is believed to show that a gap exists at this depth; it lies in the second region of heat flux in which the low heat flux is also considered indicative of a shrinkage gap. The discoloration could not, however, be correlated with the liquid pool profile any more closely than this.

In the third region the measured mould temperature 6 mm in from the face was in the range 100 to 150°C. The heat flux through the mould thus ranged from 0.4 to 1.4 MW. m^{-2}, so that the flux absorbed directly by water, which comes from spray directed towards the surface approximately 350 mm from the top of the mould, obtained by difference, ranges from about 2 to 3 MW. m^{-2}. The heat transfer coefficient for transfer direct from the metal surface to the water in the third region has a lowest

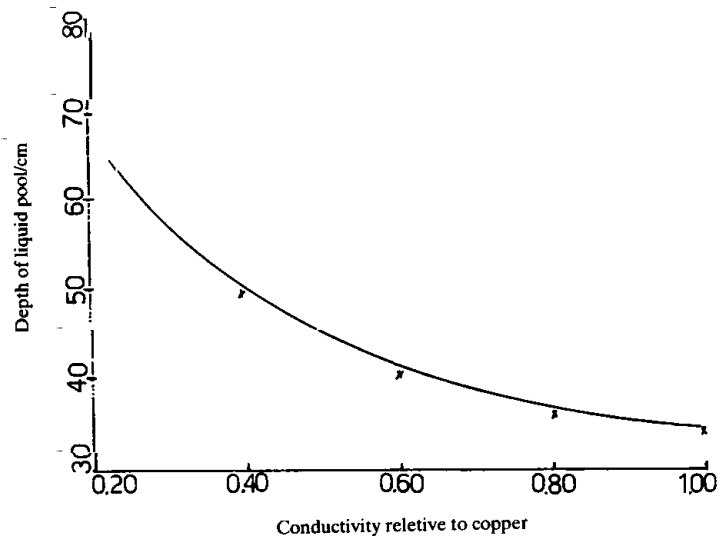

Figure 5: Effect of conductivity on liquid pool depth 650× 150 mm slab, 1088 deg.C

value of around 3 KW $m^{-2}K^{-1}$ about 250 mm from the top of the casting (at the start of the third region) where the surface temperature is around 970°C. The highest value is about 8 KW. $m^{-2}K^{-1}$ 350 mm below the top of the casting where the surface temperature is around 940°C but the casting is closer to the spray nozzles. These values are consistent with published values for cooling by water sprays [6].

NUMERICAL RESULTS

The effects on the liquid pool profile of variations in liquid metal temperature, casting speed and metal conductivity were investigated. The effects can be conveniently expressed through the depth of the liquid pool. The effect of incoming metal temperature in the range 1088°C to 115°C was not significant. The effects of casting speed and conductivity are shown in figures 4 and 5. These predictions are qualitatively reasonable but since they are based on values fitted from one set of conditions it would be desirable to test them against experimental measurements.

CONCLUSIONS

Understanding of the casting process has been significantly extended by this combination of experimental and analytical work. One unexpected finding was the very distinct separation of heat transfer into three regimes as can be seen from the experimental profile shown together with the computed profile in figure 6. The zones are interpreted as being associated with intimate contact between metal and mould, with the development of a gap between metal and mould and with the penetration of the water spray into the gap, merging into a full spray-cooled region.

The importance of spray cooling is strikingly evident in the liquid pool profiles shown in the attachment. The good general agreement between the heat transfer coefficients fitted for this region with published values for water spray cooling contributes to confidence in this aspect of the modelling. The effects of changing the water sprays could well be investigated computationally. The effect on the penetration of water into the metal mould gap immediately above the sprays can, however, only be checked experimentally.

The computational experiments treated the boundaries between these heat transfer regimes as fixed. This was necessary in the absence of additional evidence but it is possible that they change with casting conditions,

Now, according to Hamilton's principal, we set the variation of the total energy of the element equal to zero, that is

$$\delta (U-T) = 0 \qquad \int_{t_1}^{t_2} \left\{ [K]^e v + [M]^e \ddot{v} - P^e \right\} dt = 0. \qquad (23)$$

In which

$$[K]^e = [D]^e + [S]^e \qquad (24)$$

and

$$P^e = P^e{}_{fix} + P^e{}_{end} \qquad (25)$$

Where $[K]^e$ is the element stiffness matrix and $[M]^e$ is the element mass matrix.

EARTHQUAKE ANALYSIS

When a structure is excited by an earthquake, its supports have a transient motion impressed upon them. A complete special motion involves three translations and three rotations at every support. The support motion is often defined as a set of acceleration versus time values. This is the way in which the original information about a ground movement is derived from the instrument recordings. The acceleration versus time histories at the supports can be integrated to give velocity and the displacement time histories at the supports can be integarated to give velocity and the displacement time histories.

In the previous section, the FE equation of the spatial rod system was developed. By assembling the element matrices, and by implementing the boundry conditions, a set of nonhomogeneous linear system of equations is obtained. The discretized form of system equation, which is the Euler-Lagrange equation related to (23), is thus written in the form

$$[M]\ddot{v}(t) + [K]v(t) = P(t),$$

In the above equation, [M], [K] and P(t) repesent the system stiffness matix, the system mass matrix, and the system nodal force vector (at the instant t), respectively. v(t) and $\ddot{v}(t)$ designate the nodal displacement and the nodal acceleration vectors, respectively. If the structure is assumed to be subjected to an acceleration of $\ddot{v}^g(t)$ at the supports, then the vibration of such a structure can be written as

$$[M]\ddot{v}^t(t) + [K]\ddot{v}^g(t) = 0, \qquad (27)$$

in which

$$\ddot{v}^t(t) = \ddot{v}(t) + r\ddot{v}^g(t).$$

In the above relations, $\ddot{v}^t(t)$ is the total nodal acceleration of the system; it is made up of the relative nodal acceleration $\ddot{v}(t)$ and the ground acceleration $\ddot{v}^g(t)$. It is to be noted that the inertial force created in the element of the structure is proportional to the total motion of the structure, whereas the elastic forces are merely proportional to the relative motions. The vector r in equation (28) is called the influence vector and signifies the direction of the earthquake [11]. If we insert the total displacements in terms of the relative and the ground acceleration in equation (27), we obtain:

$$[M]\ddot{v}(t) + [K]v(t) = -[M]r\ddot{v}^g(t). \qquad (29)$$

In an alternative version, the above equation can be written in the form:

$$[M]\ddot{v}(t) + [K]v(t) = P(t), \qquad (30)$$

where

$$P(t) = -[M]r\ddot{v}^g(t). \qquad (31)$$

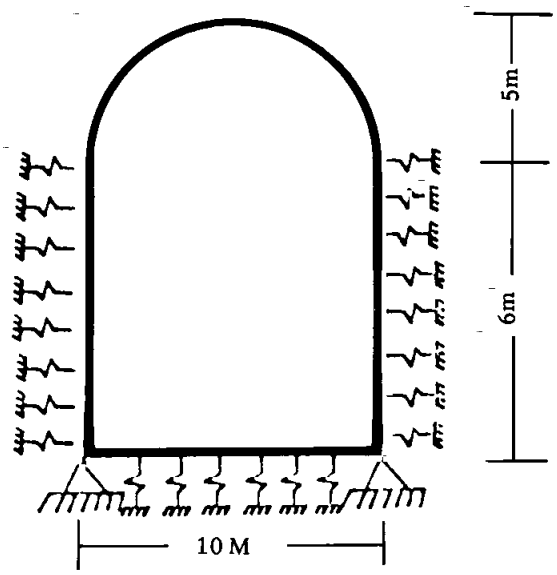

Figure 4. An arched frame on elastic foundation

To solve the nonhomogeneous system of differential equations (30), one of several techniques may be chosen. Two such methodologies include the so-called "direct integration methods" and the "method of modal superposition" [2]. The direct integration methods include: the method of central differences, the Houbolt method, the Wilson method, and the Newmark method [2]. In the present work, the Newmark method shall be used in the subsequent analysis.

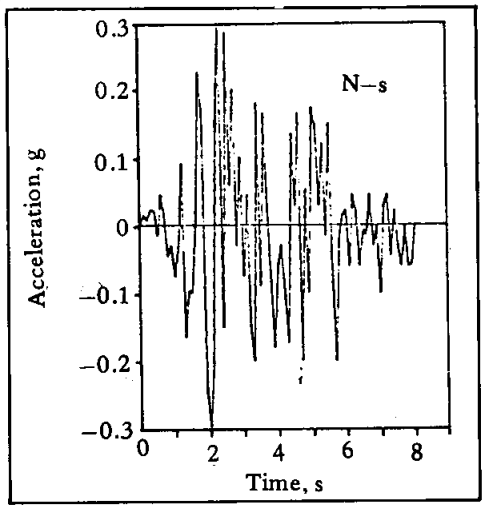

Figure 6. N–S component acceleration trace of El-Centro 1942 earthquake

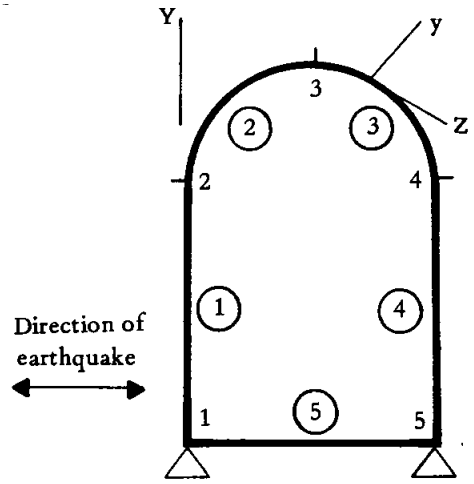

Figure 5. Discretization of the frame

THE COMPUTER PROGRAM

The numerical scheme developed in the present work is composed of two stages. One is the finite element spatial discretization and the other subsequent stage of numerical analysis corresponds to the step-wise time integration.

Based on the above-mentioned strategy, a fairly general computer program called ISAR3 is developed. This is the third program in the emerging sequence of the program ISAR. The program's members of this collection have been successfully developed and applied to static analysis and stability analysis of spatial rods [4, 5, 6, 8, 9].

ILLUSTRATIVE EXAMPLES

To show and verify the present FE model and the related computer program, the following earthquake problems are worked out.

An Arched Frame on Elastic Foundation

A semi-embedded arched frame i. e. an arch frame partially supported by an elastic foundation and subjected to an excitation record magnified to 1. 5 times. El-Centro,

(2) E.A. Mizikar, Transactions of the Metallurgical Society of AIME, Vol. 239, 1747-1753 (1969).
(3) A.W.O. Hills: *J.Iron Steel Inst.*, Vol.4, No. 2, 42-47 (1965).
(4) Elliot, C.M. & Ockendon, J.R.: Weak and variational methods for moving boundary problems, Pitman Pub., 43-47 (1982).
(5) Ockendon, Ed. and Hogkins, F.: The mathematical formulation of Stefan problems in moving boundary problems in heat flow and diffusion. Oxford University Press, 120-137 (1975).
(6) Bamberger, M. and Prinz, B.: Determination of heat transfer coefficients during water cooling at metals. *Materials Science & Technology*, Vol.2. 410-415 (1986).
(7) G.J. Davies and Y.K. Shin: Solidification technology in the foundry and casthouse, *The Metals Society, London*, 517 (1983).
(8) T. Nozaki et al., *Trans.I.S.I.J.*, Vol. 18, 330 (1978).
(9) H.R. Muller and R. Jeschar,:Z. *Metallkd, Vol. 74, 257-264 (1983).*
(10) A report from Townsville Copper Refineries, Pty. Ltd., March 1987.
(11) Alan Fine & Gordon H. Geiger,: Handbook of material and Energy Balance Calculations in Metallugical Processes, TMS-AIME, 415, (1979).
(12) Metals Handbook, Vol. 1. Properties and Selection of Metals, 8th edition, (1961).